Quantitative characterization of the microstructure and transport properties of biopolymer networks

2012 Phys. Biol. 9 036009

(http://iopscience.iop.org/1478-3975/9/3/036009)

Phys. Biol. **9** (2012) 036009 (13pp) doi:10.1088/1478-3975/9/3/036009

Quantitative characterization of the microstructure and transport properties of biopolymer networks

Yang Jiao[1] **and Salvatore Torquato**[1,2,3,4,5,6]

[1] Physical Science in Oncology Center, Princeton Institute for the Science and Technology of Materials, Princeton University, Princeton, NJ 08544, USA
[2] Department of Chemistry, Princeton University, Princeton, NJ 08544, USA
[3] Department of Physics, Princeton University, Princeton, NJ 08544, USA
[4] Princeton Center for Theoretical Science, Princeton University, Princeton, NJ 08544, USA
[5] Program in Applied and Computational Mathematics, Princeton University, Princeton, NJ 08544, USA

E-mail: torquato@princeton.edu

Received 15 March 2012
Accepted for publication 25 April 2012
Published 8 June 2012
Online at stacks.iop.org/PhysBio/9/036009

Abstract

Biopolymer networks are of fundamental importance to many biological processes in normal and tumorous tissues. In this paper, we employ the panoply of theoretical and simulation techniques developed for characterizing heterogeneous materials to quantify the microstructure and effective diffusive transport properties (diffusion coefficient D_e and mean survival time τ) of collagen type I networks at various collagen concentrations. In particular, we compute the pore-size probability density function $P(\delta)$ for the networks and present a variety of analytical estimates of the effective diffusion coefficient D_e for finite-sized diffusing particles, including the low-density approximation, the Ogston approximation and the Torquato approximation. The Hashin–Strikman upper bound on the effective diffusion coefficient D_e and the pore-size lower bound on the mean survival time τ are used as benchmarks to test our analytical approximations and numerical results. Moreover, we generalize the efficient first-passage-time techniques for Brownian-motion simulations in suspensions of spheres to the case of fiber networks and compute the associated effective diffusion coefficient D_e as well as the mean survival time τ, which is related to nuclear magnetic resonance relaxation times. Our numerical results for D_e are in excellent agreement with analytical results for simple network microstructures, such as periodic arrays of parallel cylinders. Specifically, the Torquato approximation provides the most accurate estimates of D_e for all collagen concentrations among all of the analytical approximations we consider. We formulate a universal curve for τ for the networks at different collagen concentrations, extending the work of Torquato and Yeong (1997 *J. Chem. Phys.* **106** 8814). We apply rigorous cross-property relations to estimate the effective bulk modulus of collagen networks from a knowledge of the effective diffusion coefficient computed here. The use of cross-property relations to link other physical properties to the transport properties of collagen networks is also discussed.

1. Introduction

Biopolymer networks, such as the cross-linked bundles (or fibers) of collagen and fibrin in the extracellular matrix (ECM), provide mechanical support for cells and serve as the media for the transmission of many biomechanical/biochemical cues that regulate cell motility, proliferation, differentiation and apoptosis [1–4]. The diffusion and absorption of various macromolecules in biopolymer networks are of crucial importance to the regulation and metabolism of normal organs

[6] Author to whom any correspondence should be addressed.

and to the delivery of drugs in tumor tissues [5, 6]. Such biological processes are largely determined by the composition and microstructure of the network, especially the complex pore space between the fibers [7, 8]. Thus, knowledge of the effective transport and mechanical properties of biopolymer networks is crucial in order to understand quantitatively the aforementioned biological processes.

The microstructure of biopolymer networks and their associated transport properties have been investigated by many researchers. For example, Ogston *et al* [9, 10] introduced the idea of 'influence cylinders' associated with each fiber in the system, which enables one to obtain the probability distribution of spherical pores with different sizes δ, i.e. the *pore-size probability density function* $P(\delta)$ (also referred to as the *pore-size distribution function* in the literature; see the definition in section 2). For polymer networks composed of very long and stiff fibers, Ogston derived an analytical expression of $P(\delta)$, which depends on the volume fraction and the characteristic diameter of the fibers [9]. Other approaches used to ascertain pore-size statistics include Fourier analyses of three-dimensional (3D) confocal microscopy images [11], or statistical analysis of nearest points on collagen fibers obtained from confocal-microscopic image stacks [12]. Recently, a method based on the direct analysis of the entire 3D real-space network geometry from high-contrast confocal microscopy data has been developed [13, 14]. Specifically, Lindström *et al* [14] represented the collagen fibers in the networks as thinned skeletal center lines and the cross links are represented as nodes, which can be thought of as the 'graph' representation of a biopolymer network. These authors also employed an inverse reconstruction method to characterize the microstructure of the collagen networks and investigated the mechanical properties of the networks using finite-element analysis.

The determination of the effective diffusion coefficient D_e for polymer networks dates back to the pioneering work of Johansson, Löfroth and coworkers [15–19]. Johansson *et al* experimentally studied the diffusion of small monodisperse polyethylene glycols [15] and nonionic micelles [16] in polymer systems and accurately measured the long-time-limit self-diffusion coefficient (i.e. D_e) using a tracer technique [17]. By considering the local diffusion of a particle around a single fiber, Johansson *et al* [18] derived an analytical approximation of D_e that incorporates the microstructural information of the pore space. Since their approach was based on the key concept of the distribution of 'influence cylinders' introduced by Ogston, the approximation of D_e is henceforth referred to as the Ogston approximation. To test the predictive capacity of their theory, Johansson and Löfroth [19] carried out hard-sphere Brownian-motion simulations, in which the diffusing particles were hard spheres and the fibers were considered to hinder the diffusion of the particles. Although hydrodynamic effects were not taken into account in their simulations, the results were shown to be in excellent agreement with experimental data and theoretical predictions for a wide range of particle sizes [19]. Recently, the effects of the anisotropy of fiber orientations [20, 21] and of the hydrodynamic interactions between the particle and fibers [22] on the effective diffusion coefficient have also been investigated. We note that by mathematical analogy, the problem of macromolecular diffusion in the pore space exterior to the collagen fibers is equivalent to the electrical or thermal conduction problem in the pore space with perfectly insulating fibers [23].

Very recently, it has been suggested that the powerful theoretical and simulation techniques developed for characterizing the microstructure and effective properties of random heterogeneous materials [23–26] could be fruitfully employed to model complex biological systems, especially malignant tumors and the associated host microenvironment [27]. This idea has led to fruitful applications in the understanding of the spatial organizations of abnormal cells in brain tumors [28].

In this paper, we further explore these techniques from the theory of heterogeneous materials by investigating the microstructure and transport properties of collagen type I networks (i.e. the most abundant collagen of the human body found in tissue and bones, and therefore called 'type I'; see figure 1). There exist analytical expressions that relate the effective transport and mechanical properties of general heterogeneous materials to their microstructure via a variety of n-point correlation functions; see [23] and references therein. This formalism has led to the evaluation of effective transport and mechanical properties for a variety of classes of microstructures, including dispersions of penetrable [29–31], impenetrable spheres [32–34], oriented fibers [35, 36] and ellipsoid suspensions [37, 23], fluid-saturated rocks [38] and interpenetrating ceramic-metal composites [39].

In the case of collagen-like networks, we calculate for the first time a variety of structural descriptors as well as the associated transport properties, such as the effective diffusion coefficient D_e and mean survival time τ of a Brownian particle assuming that the fiber interface is perfectly absorbing (i.e. the average time that a Brownian particle spends in the solvent before it gets trapped by the fibers). The mean survival time is related to the nuclear magnetic resonance (NMR) relaxation times as discussed below. The latter transport property is intimately related to the pore statistics [23, 40]. We also employ a variety of approximation schemes for the effective diffusion coefficient D_e, including the low-density approximation [23], Ogston approximation [18] and the Torquato approximation based on the perturbation (phase-property contrast) expansion of D_e [41, 23]. These approximations incorporate different levels of microstructural information in terms of various lower-order correlation functions that statistically describe the network microstructure. The Hashin–Strikman (HS) upper bound on the effective diffusion coefficient D_e [42] and the pore-size lower bound on the mean survival time τ [40, 43] are used as benchmarks to test our analytical approximations as well as numerical simulations. Specifically, we generalize the efficient first-passage-time (FPT) techniques for Brownian-motion simulations in suspensions of spheres [44–48] to the case of fiber networks and compute the associated effective diffusion coefficient D_e and mean survival time τ. Our numerical results of D_e are in excellent agreement with analytical results of simple network microstructures such as periodic arrays of parallel cylinders. Moreover, we show that the Torquato approximation provides the most

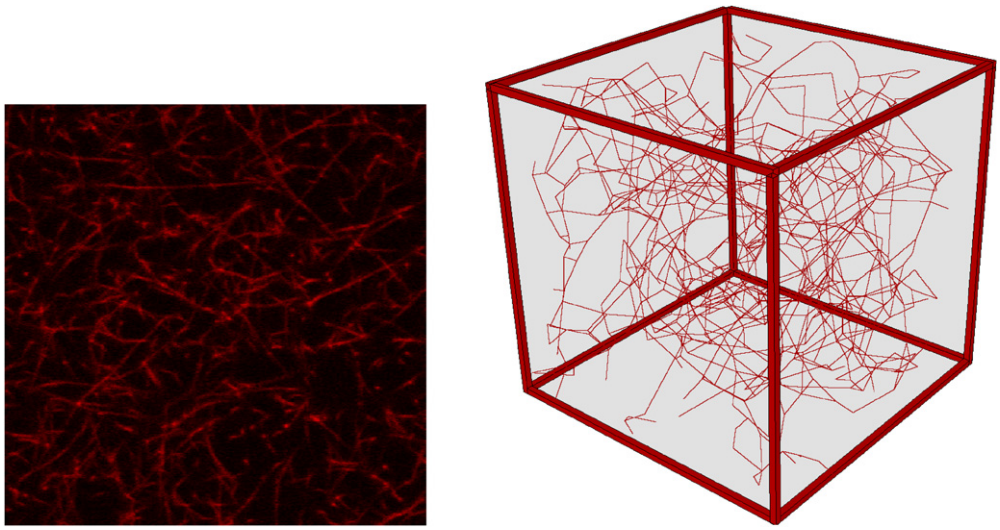

(*a*) (*b*)

Figure 1. Collagen networks. (*a*) Confocal microscope image of collagen-I at a final collagen concentration 2.0 mg ml^{-1}. The linear size of the image is approximately 150 μm. Image courtesy of S B Lindström. (*b*) Three-dimensional 'graph' representation of the collagen network studied here. The linear size of the box is approximately 100 μm.

accurate estimate of D_e for all collagen concentrations among the employed approximation schemes. We also formulate a universal curve for τ for different networks at different collagen concentrations, i.e. we devise a way to scale τ in such a way that the scaled data for different collagen networks collapse onto a single curve. Rigorous cross-property relations [23] are applied to estimate the effective bulk modulus of collagen networks from a knowledge of the computed effective diffusion coefficient.

The rest of the paper is organized as follows. In section 2, we define the statistical descriptors that will be used to characterize the network microstructures. In section 3, we provide analytical approximations and rigorous bounds for the effective properties D_e and τ. In addition, we discuss the FPT simulation techniques for network structures in detail. In section 4, we present the analytical and numerical results of the correlation functions and the effective transport properties. In section 5, we estimate the effective bulk modulus of collagen networks using the cross-property relations from the computed effective diffusion coefficients of the networks. In section 6, we make concluding remarks, including the use of cross-property relations to link other physical properties to the transport properties of collagen networks.

2. Network microstructure characterization

A collagen network can be considered to be a two-phase heterogeneous material composed of a fiber phase and a solvent phase (i.e. the pore space), which is exterior to the fibers. An important feature of such a network microstructure is that both phases percolate across the system, i.e. there is a continuous path between any two points of the phase of interest that is entirely in the phase of interest, even when the volume fraction of the fiber phase (fraction of space covered by the fibers) is very low. In this section, we introduce various statistical microstructural descriptors for a general two-phase material, including the n-point correlation functions S_n and the pore-size probability density function $P(\delta)$.

2.1. *n-point correlation functions*

Consider a two-phase heterogeneous material in which each phase has the volume fraction ϕ_i ($i = 1, 2$); it is customary to introduce the indicator function $\mathcal{I}^{(i)}(\mathbf{x})$ defined as

$$\mathcal{I}^{(i)}(\mathbf{x}) = \begin{cases} 1, & \mathbf{x} \in \mathcal{V}_i, \\ 0, & \mathbf{x} \in \bar{\mathcal{V}}_i, \end{cases} \tag{1}$$

where $\mathcal{V}_i$ is the region occupied by the phase i and $\bar{\mathcal{V}}_i$ is the region occupied by the other phase. The statistical characterization of the spatial variations of the material involves the calculation of the standard n-point correlation functions:

$$S_n^{(i)}(\mathbf{x}_1, \mathbf{x}_2, \ldots, \mathbf{x}_n) = \langle \mathcal{I}^{(i)}(\mathbf{x}_1)\mathcal{I}^{(i)}(\mathbf{x}_2)\cdots\mathcal{I}^{(i)}(\mathbf{x}_n)\rangle, \tag{2}$$

where the angular brackets $\langle\cdots\rangle$ denote an ensemble average. The quantity $S_n^{(i)}(\mathbf{x}_1, \mathbf{x}_2, \ldots, \mathbf{x}_n)$ also gives the probability of finding n points positioned at $\mathbf{x}_1, \mathbf{x}_2, \ldots, \mathbf{x}_n$ all in phase i.

For *statistically homogeneous* materials, the n-point correlation function depends not on the absolute positions but on their relative displacements, i.e.

$$S_n^{(i)}(\mathbf{x}_1, \mathbf{x}_2, \ldots, \mathbf{x}_n) = S_n^{(i)}(\mathbf{x}_{12}, \ldots, \mathbf{x}_{1n}), \tag{3}$$

for all $n \geqslant 1$, where $\mathbf{x}_{ij} = \mathbf{x}_j - \mathbf{x}_i$. Thus, there is no preferred origin in the system, which in equation (3) we have chosen to be the point $\mathbf{x}_1$. In particular, the one-point correlation function is a constant everywhere, namely it is equal to the volume fraction ϕ_i of the phase i, i.e.

$$S_1^{(i)} = \langle \mathcal{I}^{(i)}(\mathbf{x})\rangle = \phi_i, \tag{4}$$

which is the probability that a randomly chosen point in the material belongs to the phase i. For *statistically isotropic* materials, the n-point correlation function is invariant under rigid-body rotation of the spatial coordinates. For $n \leqslant d$, this

implies that $S_n^{(i)}$ depends only on the distances $x_{ij} = |\mathbf{x}_{ij}|$ $(1 \leqslant i < j \leqslant n)$.

In general, an infinite set of S_n with $n = 1, 2, 3...$ is required to completely determine the microstructure and, thus, the effective properties of a heterogeneous material [23]. Specifically, the effective property of interest can be written as an infinite series involving integrals of such correlation functions. In practice, a complete knowledge of all of the S_n is never available. However, it has been shown that certain approximations that can be regarded as resummations of the infinite series expansion that incorporate lower order S_n (e.g., S_2, S_3 and S_4) can provide accurate estimates of the effective properties [23]. We note that since only certain weighted integrals of the correlation functions are needed, excellent approximations of effective properties can be obtained even without computing all of the S_n explicitly. We will discuss these approximations in detail in section 3.1.

2.2. Pore-size probability density function

The pore-size probability density function $P(\delta)$ first rose to characterize the pore space in porous media [43] and was then generalized to characterize any heterogeneous material [23]. For a statistically homogeneous and isotropic material, $P(\delta)\mathrm{d}\delta$ gives the probability that a randomly chosen point in the pore space lies at a distance between δ and $\delta + \mathrm{d}\delta$ from the nearest point on the pore–solid interface. Since it is a probability density function with dimensions of inverse length, we have $P(\delta) \geqslant 0$ for all δ, and it normalizes to unity, i.e.

$$\int_0^\infty P(\delta)\,\mathrm{d}\delta = 1. \tag{5}$$

At extreme values of $P(\delta)$, we have that

$$P(0) = s/\phi_1, \quad P(\infty) = 0, \tag{6}$$

where s is the pore–solid interface area per unit volume and ϕ_1 is the volume fraction of the pore space. Therefore, s/ϕ_1 is the interface area per unit pore volume. The moments of $P(\delta)$, defined as

$$\langle \delta^n \rangle = \int_0^\infty \delta^n P(\delta)\,\mathrm{d}\delta, \tag{7}$$

provide useful characteristic length scales of the pore space in the material. Certain lower order moments of $P(\delta)$ also arise in bounds on the mean survival time τ [43, 40], which we will discuss in section 3.

It is very difficult to obtain the analytical expression of $P(\delta)$ for a general polymer network. For networks composed of very long and stiff polymer fibers, Ogston [9] derived an expression for $P(\delta)$, i.e.

$$P(\delta) = \frac{2\phi_2(\delta + a)}{a^2}\,\mathrm{e}^{-\phi_2(\delta+a)^2/a^2}, \tag{8}$$

where $\phi_2 = 1 - \phi_1$ is the volume fraction of the fibers and a is the fiber radius. For $\delta = 0$, equation (8) gives

$$P(0) = s. \tag{9}$$

Comparing equations (9) and (6), it is clear that the Ogston expression for $P(\delta)$ can only provide good estimates of it at very low fiber volume fractions, i.e. $\phi_2 \to 0$ and $\phi_1 = 1 - \phi_2 \approx 1$. In general, the Ogston expression will overestimate $P(\delta)$ at intermediate δ, as we will show in section 4.

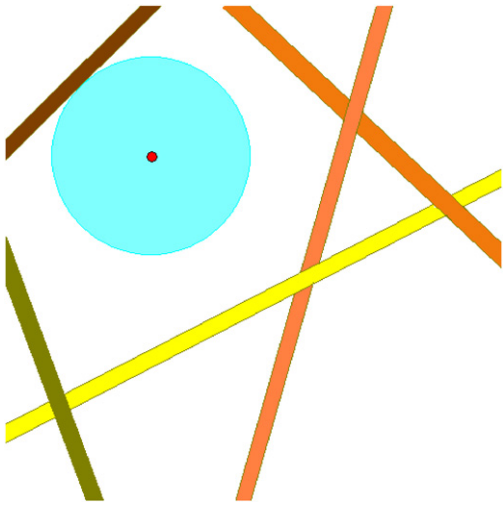

Figure 2. A schematic showing of how to sample the pore-size probability density function $P(\delta)$ of a collagen network in two dimensions. Shown are thin fibers that can possibly intersect as well as a randomly selected test point in the pore space (red) and its associated largest sphere (blue) that just touches the nearest fiber.

Given any network microstructure, the associated $P(\delta)$ can be numerically computed. Specifically, one generates many test points that are randomly distributed in the pore space exterior to the fibers and computes the distances from each test point to the nearest fiber surface. This amounts to finding the largest test sphere centered at a randomly selected test point that is entirely in the pore space; see figure 2. The resulting distances are binned to obtain a probability density function, which is then normalized to give $P(\delta)$ [23].

3. Mean survival time and effective diffusion coefficient

3.1. Theoretical techniques

3.1.1. Mean survival time. Consider the steady-state problem of diffusion of macromolecules which are absorbed upon contacting the network fibers. This implies that the rate of production of the macromolecules per unit volume G is exactly compensated by the rate of removal by the traps. Locally, the process is described by the following Poisson equation [23]:

$$D_1 \Delta c = -G \text{ in } \mathcal{V}_1, \quad c = 0 \text{ on } \partial\mathcal{V}, \tag{10}$$

where c is the concentration of the macromolecule, D_1 is the diffusion coefficient of the macromolecule in the pore space $\mathcal{V}_1$ and $\partial\mathcal{V}$ is the pore–fiber interface. The boundary condition that $c = 0$ on $\partial\mathcal{V}$ assumes a perfectly absorbing interface, i.e. a diffusion-controlled reaction. This boundary condition can easily be relaxed to take into account partially absorbing interfaces [23, 40].

An important quantity is the mean survival time τ associated with a macromolecule which is the average time that a diffusing macromolecule spends in the pore space before it gets trapped by the fibers. In many medical applications, the efficiency of a drug strongly depends on the ability of

the drug macromolecules to diffuse through the extracellular space mainly composed of collagen without getting trapped by the fibers [5]. It is noteworthy that NMR relaxation in porous media, a widely used technique for biomedical imaging, yields NMR relaxation times from which one can extract the mean survival time we consider here [23].

The mean survival time τ is inversely proportional to the trapping constant γ, i.e.

$$\tau = \frac{1}{\gamma \phi_1 D_1}, \tag{11}$$

where γ is defined via

$$G = \gamma D_1 \langle c \rangle, \tag{12}$$

where $\langle c \rangle$ is the ensemble-averaged concentration field.

The optimal lower bound on the mean survival time τ that incorporates information on the pore space in terms of the first moment of the pore-size probability density function is given by [40, 43]

$$\tau \geqslant \frac{\langle \delta \rangle^2}{D_1}, \tag{13}$$

where $\langle \delta \rangle = \int_0^\infty \delta P(\delta)\, \mathrm{d}\delta$. It can be seen from equation (13) that τD_1 can provide an estimate of the average pore size of the network. A corresponding upper bound on the trapping constant can be obtained by substituting equation (11) into equation (13).

3.1.2. Effective diffusion coefficient. Consider macromolecules diffusing between the fibers that are not absorbed by the fibers. The Brownian motions of the macromolecules are hindered by the fibers in the network which results in an effective diffusion coefficient D_e smaller than that of the pure solvent in the pore space D_1. By mathematical analogy, the problem of macromolecular diffusion in the pore space exterior to the fibers is equivalent to the electrical or thermal conduction problem in the pore space with perfectly insulating fibers. Specifically, the local 'flux' $\mathbf{J}(\mathbf{x})$ of macromolecules is proportional to a local 'intensity' $\mathbf{E}(\mathbf{x})$ which is the negative gradient of the macromolecule concentration field $c(\mathbf{x})$, i.e.

$$\mathbf{J}(\mathbf{x}) = \mathbf{D}(\mathbf{x}) \cdot \mathbf{E}(\mathbf{x}) = -\mathbf{D}(\mathbf{x}) \cdot \nabla c(\mathbf{x}), \tag{14}$$

where

$$\mathbf{D}(\mathbf{x}) = \begin{cases} D_1 \mathbf{I}, & \mathbf{x} \in \mathcal{V}_1 \\ 0, & \text{otherwise} \end{cases} \tag{15}$$

and $\mathbf{I}$ is the unit second-order tensor. Under steady-state conditions with no source and sink terms, the conservation of macromolecules requires that $\mathbf{J}(\mathbf{x})$ be solenoidal [23], i.e.

$$\nabla \cdot \mathbf{J}(\mathbf{x}) = 0. \tag{16}$$

If $\mathbf{D}(\mathbf{x})$ in equation (14) is replaced by the local conductivity tensor $\sigma(\mathbf{x})$, one obtains the local governing equations for conduction problems. We would like to emphasize that although the diffusion problem and conduction problem are equivalent in their mathematical formulations, there is an important distinction between the effective diffusion coefficient D_e and the effective conductivity σ_e. For the conduction problem, although the fiber phase is insulating, its contribution to σ_e is still explicitly considered. For example, suppose that one randomly places test particles and tracks their Brownian motions to compute σ_e. There is a fraction of total number of particles ϕ_2, which are initially in the insulating fiber phase and will be trapped there forever. Clearly these test particles, which have a zero diffusion coefficient, are taken into account in the ensemble average for σ_e. On the other hand, only the test particles in the pore space are considered in order to compute D_e. Therefore, D_e and σ_e for the same microstructure are related to one another via the following relation:

$$\frac{D_e}{D_1} = \frac{1}{\phi_1}\frac{\sigma_e}{\sigma_1} = \frac{1}{(1-\phi_2)}\frac{\sigma_e}{\sigma_1}. \tag{17}$$

In the following, we present rigorous bounds and various analytical approximations for the effective diffusion coefficient D_e. These results were reported in the literature for the effective conductivity σ_e of a general heterogeneous material. Here, we modify them according to equation (17) to obtain expressions for D_e.

Hashin–Strikman (*HS*) *upper bound.* For a two-phase heterogeneous material with an arbitrary but isotropic microstructure in which one of the phases (e.g., phase 2) is insulating, the HS upper bound for the effective diffusion coefficient D_e is given by

$$\frac{D_e}{D_1} = \frac{2}{2+\phi_2}. \tag{18}$$

The HS lower bound in this case is trivially zero for all values of ϕ_2 [23].

Although only volume fractions explicitly appear in the expression, it has been shown that the HS bound is the optimal bound given the two-point information of the isotropic microstructure, i.e. S_2 [23]. Specifically, it is shown that the HS bounds are realizable for a special class of 'coated sphere' model microstructures [23]. However, it is clear that such two-point information is far from a complete characterization of the network microstructure. Therefore, it can be expected that the HS upper bound is not tight, as we will show in section 4.

Low-density approximation. For a heterogeneous material with microstructure composed of well-defined inclusions (such as spheres, ellipsoids or cylinders) in a matrix, the effective properties of the material can be written as a power series of the volume fraction ϕ_2 of the inclusions [23]. When ϕ_2 is sufficiently small, i.e. in the low-density limit, truncating the power series through the first order in ϕ_2 can provide a reasonable estimate of the effective properties of interest.

For fiber networks, we consider that each fiber is an elongated prolate spheroid in the 'needle' limit. In such cases, the effective diffusion tensor for dilute suspensions of orientated needles is given by

$$\mathbf{D}_e = \begin{bmatrix} (D_e)_{11} & 0 & 0 \\ 0 & (D_e)_{22} & 0 \\ 0 & 0 & (D_2)_{33} \end{bmatrix}, \tag{19}$$

where

$$\begin{aligned} (D_e)_{11} = (D_e)_{22} &= D_1\left[1 - \phi_2 + O\left(\phi_2^2\right)\right], \\ (D_e)_{33} &= D_1\left[1 + O\left(\phi_2^2\right)\right]. \end{aligned} \tag{20}$$

For statistically isotropic materials such as suspensions of randomly orientated needles in a matrix, the effective diffusion

coefficient is the average of the three principal components of the tensor $\mathbf{D}_e$, i.e.

$$\frac{D_e}{D_1} = 1 - \frac{2}{3}\phi_2 + O(\phi_2^2). \tag{21}$$

Physically, equation (21) corresponds to the diffusion of Brownian particles in a matrix with a single infinitely long fiber, which clearly overestimates D_e for actual biopolymer networks. However, for certain microstructures such as periodic arrays of parallel cylinders at low volume fractions, equation (21), which we call the *low-density approximation*, can provide accurate estimates of D_e, which can be used as benchmarks to test our simulation results.

Ogston approximation. An improved approximation for D_e over the aforementioned low-density approximation can be obtained if the contributions of multiple fibers are taken into account simultaneously. This can be done by using the idea of an 'influence cylinder' associated with each fiber introduced by Ogston [10]. Specifically, consider a 'coated cylinder' with outer radius b and inner radius a (i.e. the radius of the fiber). One can easily compute the local effective diffusion coefficient $D_L(b)$ associated with the coated cylinder, i.e.

$$\frac{D_L(b)}{D_1} = \frac{1}{1 + a^2/b^2} = \frac{1}{1 + \phi_2(b)}, \tag{22}$$

where $\phi_2(b)$ is local volume fraction of the fiber in the coated cylinder.

Now consider that the global D_e of a network is a weighted average of the local $D_L(b)$ for the influence cylinders associated with each fiber, which leads to the relation

$$\frac{D_e}{D_1} = \int_a^\infty f(b)\frac{D_L(b)}{D_1}\,\mathrm{d}b, \tag{23}$$

where $f(b)$ is the influence cylinder distribution function [18]. Ogston and coworkers assume that the influence cylinders contribute to the global D_e in the same way they contribute to the pore-size probability density function $P(\delta)$, i.e.

$$P(\delta) = \int_a^\infty f(b)g(b,\delta)\,\mathrm{d}b, \tag{24}$$

where $g(b, \delta)$ is the local pore-size distribution associated with a coated cylinder with outer radius b given by

$$g(b,\delta) = \frac{2(a+\delta)}{b^2}H[\delta - (b-a)] \tag{25}$$

and $H(x)$ is the Heaviside step function, equal to unity for $x > 0$ and zero otherwise. Then $f(b)$ can be obtained by deconvolution of equation (24) with a knowledge of $P(\delta)$, either from direct numerical sampling or theoretical considerations.

Torquato approximation. Torquato has derived an infinite series expansion of the effective conductivity σ_e of any two-phase heterogeneous materials in terms of the contrast between the conductivities of the individual phases that he called the 'strong-contrast' expansion [41]. He showed that a certain approximate but accurate resummation of the 'strong-contrast' expansion of the effective conductivity σ_e, which incorporates up to four-point microstructural information involving integrals over S_2, S_3 and S_4, can provide excellent estimates of σ_e for a wide range of model microstructures [41]. This resummation is the [2,2] Padé (i.e. rational function) approximant of the 'strong-contrast' expansion [41, 23].

Here, we present the modified four-point [2, 2] Padé approximation of the effective diffusion coefficient D_e for collagen networks, which is henceforth referred to as the Torquato approximation, i.e.

$$\frac{D_e}{D_1} = \frac{1}{1-\phi_2}\frac{\left(1 + \frac{1}{2}\frac{\gamma_2}{\zeta_2} - \frac{1}{2}\zeta_2\right) + \left(-1 + \frac{1}{2}\zeta_2 - \frac{1}{2}\frac{\gamma_2}{\zeta_2}\right)\phi_2}{\left(1 + \frac{1}{2}\frac{\gamma_2}{\zeta_2} - \frac{1}{2}\zeta_2\right) + \left(\frac{1}{2} + \frac{1}{2}\zeta_2 + \frac{1}{4}\frac{\gamma_2}{\zeta_2}\right)\phi_2}, \tag{26}$$

where the parameter ζ_2 is a weighted integral that involves the correlation functions S_1, S_2 and S_3 of the fiber phase, and the parameter γ_2 is a weighted integral that involves the correlation functions S_1, S_2, S_3 and S_4 of the fiber phase. The readers are referred to [41] for detailed discussions of these parameters. Useful rigorous inequalities relating ζ_2 and γ_2 for three-dimensional microstructure are as follows [41]:

$$-1 \leqslant \gamma_2/\zeta_2 \leqslant 1 - 2\zeta_2. \tag{27}$$

It is in general nontrivial to compute the three-point and four-point correlation functions S_3 and S_4, even for relatively simple model microstructures (e.g., dispersions of spheres), to obtain exact values of ζ_2 and γ_2. However, it has been shown that simplified estimates of these parameters based on limited microstructural information in conjunction with equation (26) can lead to excellent approximations for the effective properties [41, 23]. Here, we consider the low-density approximation of ζ_2 for a prolate spheroid in the needle limit and only keep the leading-order term, i.e. $\zeta_2 = 1/4$ [23]. The inequalities given in equation (27) then become

$$-1 \leqslant \gamma_2/\zeta_2 \leqslant 1/2. \tag{28}$$

It has been shown that for dispersions of spheres, $\gamma_2 = 0$ can provide a very accurate approximation formula for the effective conductivity of a wide range of sphere volume fractions [41]. We will show in section 4 that a proper choice of γ_2 value that is near its lower bound can provide an excellent approximation for the effective diffusion coefficient associated with biopolymer networks.

3.2. First-passage-time (FPT) simulation techniques

A straightforward way of numerically studying Brownian motion is to simulate the exact zig–zag path of a diffusing particle (e.g., see [19]). However, it is clear that this direct approach is not an efficient means of obtaining effective diffusive properties, since the details of the diffusion paths are averaged out and do not contribute to the effective behavior. Moreover, one needs to consider a wide range of step sizes associated with each random Brownian jump to extrapolate the results to the case of infinitesimal small step size.

An alternative but much more computationally efficient approach is the FPT simulation technique introduced by Torquato and coworkers [44–48]. The key idea of the FPT approach is not to simulate the details of the zig–zag diffusion paths but rather consider the average time that it takes a Brownian particle to 'jump' directly to a random location on the surface of the largest imaginary sphere that is centered at the original position of the particle and entirely within the solvent (i.e. the pore phase). The imaginary sphere is

referred to as the 'first-passage sphere' (FPS), whose radius is R. It can be shown that the mean time $\tau_{\rm FPS}$ for a Brownian particle, which is initially at the center of the FPS and takes a complicated zig–zag path to hit the surface of the FPS, is, in three dimensions, given by

$$\tau_{\rm FPS} = R^2/(2\,dD_1), \tag{29}$$

where $d = 3$ is the space dimension.

When the particle is very close to the fiber surface, i.e. the distance r from the particle centroid to the fiber surface is smaller than a prescribed tolerance Δ, we consider that the particle hits the fiber surface and is reflected back. The FPS in this case encloses both the pore phase and fiber phase. Suppose that the FPS centered at the Brownian particle centroid possesses a radius R; the associated time $\tau_{\rm REF}$ that the Brownian particle takes to hit the fiber surface, be reflected back and hit the FPS can be estimated by

$$\tau_{\rm REF}(r) = \frac{R^2}{6D_1}\frac{V_1+V_2}{V_1}\left[1+\frac{1}{2}\left(\frac{r}{R}\right)^2 - \frac{1}{2}\sum_{m=0}^{\infty} C_{2m+1}\left(\frac{r}{R}\right)^{2m+1}\right], \tag{30}$$

where $0 \leqslant r \leqslant R$, V_1 and V_2 are the volume of the pore phase and the volume of the fiber phase enclosed in the FPS, respectively, and

$$C_{2m+1} = \frac{(-1)^{m+1}(2m)!}{2^{2m+1}(m!)^2}\frac{3(4m+3)}{(2m-1)(m+2)(m+1)}. \tag{31}$$

Equation (30) was first derived by Torquato and coworkers [45–47], and it has been shown to provide excellent approximation of the exact $\tau_{\rm REF}$ for any local geometry when $r \ll R$ and R is smaller than the diameter of the fiber. The readers are referred to [45] and the references therein for additional details.

To compute $\tau_{\rm REF}$ using equation (30), a key step is to evaluate the intersection volume between a sphere and a cylinder (i.e. V_2), the details of which are given in the appendix. In the rare case when the particle is close to a cross link (junction of several fibers), V_2 is the volume of the fiber junction enclosed in the FPS, which is computed by Monte Carlo sampling [47]. For example, one randomly places test points in the FPS and computes the fraction of times that the point falls into the vicinity of the fiber junction.

To obtain D_e, one considers an ensemble of Brownian trajectories in the pore space. When a diffusing particle is sufficiently far away from the fiber surface, one constructs the largest FPS of radius R around the diffusing particle which just touches the fiber surface. The particle then jumps in one step to a random point on the surface of the FPS and the process is repeated, each time keeping track of R_i^2, until the particle is within a prescribed very small distance Δ to the fiber surface (see figure 3). At this point in time, the particle is considered to hit the fiber and then is reflected back. Thus, one keeps track of the radius R_j of the FPS that encloses both the fiber phase and the pore phase and computes the associated time $\tau_{\rm REF}(R_j)$. The expression for the effective diffusion coefficient D_e is then given by

$$\frac{D_e}{D_1} = \left\langle \frac{\sum_i R_i + \sum_j R_j}{\sum_i R_i + 6D_1\sum_j \tau_{\rm REF}(R_j)} \right\rangle, \tag{32}$$

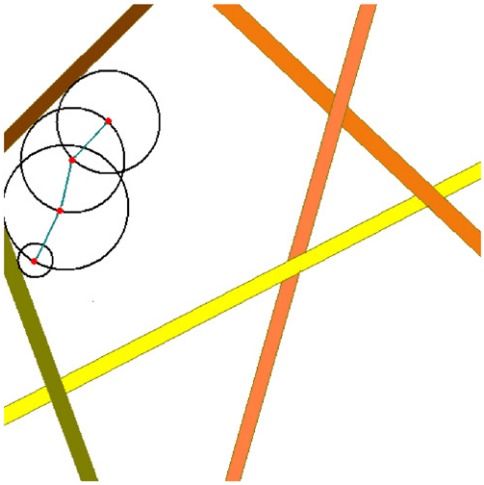

Figure 3. A schematic showing of the FPT simulation technique in two dimensions. Shown are thin fibers that can possibly intersect as well as several first-passage spheres. Starting from an initial position, a diffusing particle jumps to a random location on the surface of its associated first-passage sphere. This jumping process is repeated until the particle falls within a small tolerance distance from the fiber surface, at which point the particle is reflected back to the pore space.

where $\tau_{\rm REF}(R)$ is given by equation (30) and $\langle . \rangle$ denotes the ensemble average over many Brownian particles. In our simulations, we use $N = 5000$ Brownian particles.

The mean survival time τ can be obtained in a similar way [44]. Specifically, one constructs the FPT path composed of many jumps to the surface of FPS associated with a Brownian particle and keeps track of R_i for each FPS. When the particle is within Δ to the fiber surface, it is considered trapped by the fiber. Thus, the mean survival time can be computed via

$$\tau = \left\langle \sum_i R_i/D_1 \right\rangle, \tag{33}$$

where $\langle . \rangle$ denotes ensemble average over many Brownian particles. In our simulations, we use $N = 5000$ Brownian particles.

We note that in the aforementioned FPT simulation technique, we consider that the Brownian particle is a 'point' particle with zero diameter. For finite-sized particle diameter $d_{\rm P}$, it has been shown that one can still consider 'point' particles in a network microstructure with the diameter of the fibers $d_{\rm F}$ dilated by $d_{\rm P}$ [48, 49].

4. Results

Our data are 'graph representations' of collagen type I networks [14] with final collagen concentrations of 1.0, 2.0 and 4.0 mg ml^{-1}. The fibers roughly possess a circular cross section of diameter $d_{\rm F} = 1.0 \times 10^{-7}$ m [14]. The average fiber lengths $\ell_{\rm F}$ for the networks with the three collagen concentrations are respectively 1.96×10^{-6}, 1.81×10^{-6} and 1.28×10^{-6} m. The corresponding volume fractions of the fibers are respectively 1.7×10^{-3}, 2.4×10^{-3} and 5.2×10^{-3}. The tolerance Δ described in section 3 is chosen to be $\Delta = 5 \times 10^{-3} d_{\rm F} = 5.0 \times 10^{-10}$ m. Since we do not consider

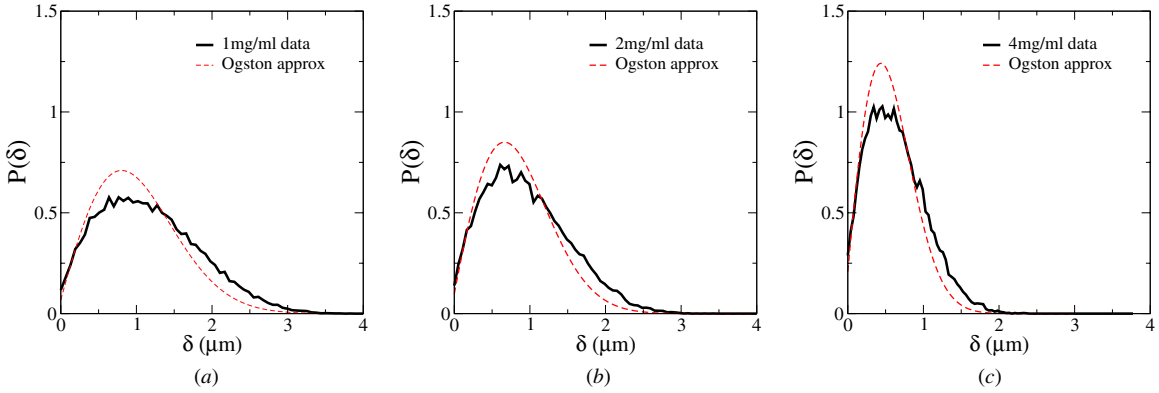

Figure 4. The pore-size probability density function $P(\delta)$ for collagen networks at different collagen concentrations.

hydrodynamic effects in our simulations, we consider only particles with diameter d_P comparable to the fiber diameter d_F, i.e. $d_P \leqslant 1.5\,d_F$. For large d_P, it has been shown that the hydrodynamic effects on Brownian motion are significant [22]. The results reported below are ensemble averages of three independent network configurations at each collagen concentration.

4.1. Pore-size probability density function

The pore-size probability density functions $P(\delta)$ for the collagen network at three concentrations are numerically computed as described in section 2. The obtained $P(\delta)$ are shown in figure 4 and compared to the corresponding Ogston expressions (equation (8)) at the same fiber volume fractions.

It can be clearly seen that the Ogston expression of $P(\delta)$ overestimates the number of intermediate pores and underestimates the number of large pores in the system. This is because in the derivation of equation (8), it is assumed that the network is composed of fibers with very long persistence length. For the collagen networks we study, the average fiber lengths ℓ are less than twice the corresponding averaged pore size $\langle\delta\rangle$ (defined in equation (7)), which are respectively 1.22×10^{-6}, 0.998×10^{-6} and 0.684×10^{-6} m for collagen concentrations 1.0, 2.0 and 4.0 mg ml^{-1}. Therefore, the long-fiber-length assumption for the Ogston expression is not true here.

The $P(\delta)$ data will be employed to compute the lower bound on the mean survival time τ (equation (13)) and to compute the Ogston approximation for the effective diffusion coefficient D_e (equation (23)) in the following sections.

4.2. Mean survival time

The mean survival time τ is computed using the FPT technique described in section 2. Figure 5 shows the scaled dimensionless mean survival time $\tau D_1/\ell_F^2$ for the collagen networks with three different concentrations as a function of Brownian particle diameter. It can be seen that as the collagen concentration increases, larger particles are more easily get trapped by the fibers. This fact is of great importance in cancer chemotherapy, which we will discuss in section 6.

As indicated in section 3, the diffusion of finite-sized particles in the original network is equivalent to the diffusion of

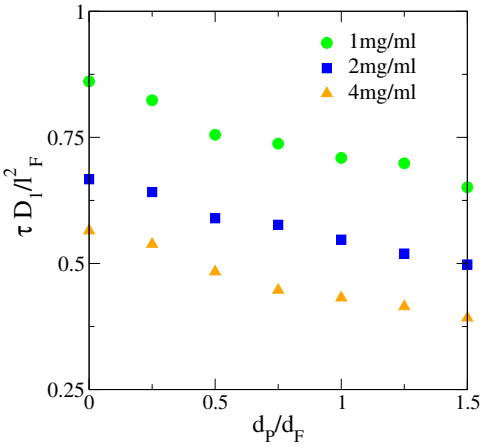

Figure 5. The scaled dimensionless mean survival time $\tau D_1/\ell_F^2$ for the collagen networks at different collagen concentrations as a function of the diffusing particle diameter, as computed from our first-time-passage simulations.

point particles in a properly dilated network, which possesses a higher fiber volume fraction. Figure 6 shows the scaled mean survival time $\tau D_1/\ell_F^2$ for the collagen networks with three different concentrations as a function of the particle diameter. The pore-size lower bounds are also shown. It can be seen that although the bounds are not sharp, they do not deviate very much from the actual mean survival times. We note that these bounds only incorporate partial information about the pore-size probability density function $P(\delta)$, namely the first moment $\langle\delta\rangle$ of $P(\delta)$. Therefore, one would expect that incorporating the full information content of $P(\delta)$ would lead to good predictions of the effective diffusive properties considered here. Indeed, we will show in the following section that the generalization of the Ogston approximation that employs the complete microstructural information contained in $P(\delta)$ provides a very good estimate of D_e.

In [50], Torquato and Yeong found a universal curve for a scaled mean survival time τ for a wide range of microstructures with different porosities, including various random and ordered distributions of spheres and certain continuous models. Specifically, the universal curve has the following form:

$$\frac{\tau}{\tau_0} = a_1 x + a_2 x^2, \tag{34}$$

where a_1 and a_2 are constants and

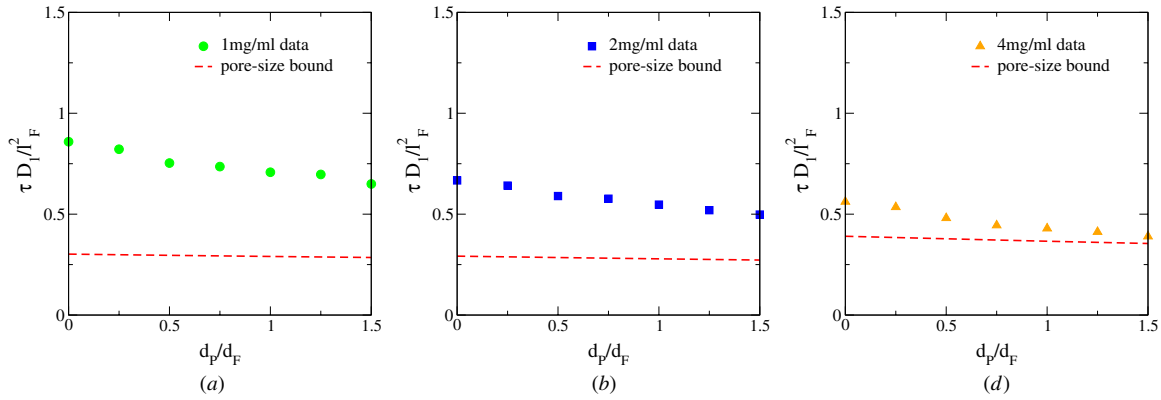

Figure 6. The scaled dimensionless mean survival time $\tau D_1/\ell_F^2$ for the collagen networks at different collagen concentrations as a function of the diffusing particle diameter and the associated pore-size lower bound.

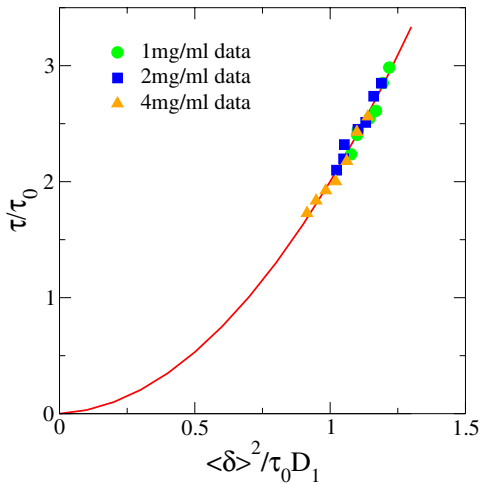

Figure 7. Universal curve for the scaled mean survival time τ/τ_0 versus $\langle\delta\rangle^2/(\tau_0 D_1)$ for the collagen networks at different collagen concentrations. It is seen that the scaled mean survival time for different collagen networks collapses onto a single curve.

$$\tau_0 = \frac{3\phi_2}{D_1\phi_1 s^2}, \quad x = \frac{\langle\delta\rangle^2}{\tau_0 D_1}, \tag{35}$$

and s is the specific surface, i.e. the solid–pore interface area per unit volume. For the class of microstructures they studied, Torquato and Yeong found that $a_1 = 8/5$ and $a_2 = 8/7$.

For the collagen networks studied here, we find that equation (34) also holds (see figure 7). However, the constants are different from those obtained by Torquato and Yeong, i.e. we find that $a_1 = 0.121$ and $a_2 = 1.88$ for the networks with different concentrations. A possible reason for the difference in the constants is that collagen networks do not belong to the same class of microstructures studied in [50], which, for example, do not contain filamentary-like structures, as in the case of collagen fibers. This implies that there could exist a more general scaling curve for the mean survival time that incorporates both the networks and the microstructures studied in [50]. Nonetheless, our results enable one to efficiently estimate the properties of collagen networks. In particular, given any of the three quantities among the four quantities τ, ϕ_1, s and $\langle\delta\rangle$, the remaining one can be estimated employing equation (34).

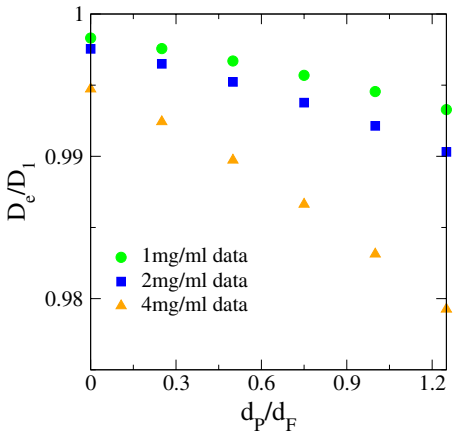

Figure 8. The dimensionless effective diffusion coefficient D_e/D_1 for the collagen networks at different collagen concentrations as a function of the diffusing particle diameter, as computed from our first-time-passage simulations.

4.3. Effective diffusion coefficient

The effective diffusion coefficients D_e for various network microstructures are computed using both the theoretical techniques described in section 3.1 and the FPT technique described in section 3.2. Figure 8 shows D_e for the fiber networks with different collagen concentrations as a function of the Brownian particle diameter. Similar to the case of the mean survival time, as the collagen concentration ϕ increases, it becomes more and more difficult for larger particles to diffuse in the collagen.

Figure 9 shows D_e as a function of the fiber volume fraction. In addition to the results for the collagen networks, we also show D_e for a model microstructure composed of parallel cylinders arranged on a square lattice. The HS upper bound and various approximations of D_e discussed in section 3.1 are also shown in figure 9. As we indicated earlier, since the HS bound only incorporates the limited two-point information S_2, it cannot provide a good estimate of D_e. This is also evident from the fact that the HS bound is realized by a certain class of 'coated sphere' model microstructures, which are clearly topologically distinct from the network microstructures because one of the phases is topologically disconnected. It can

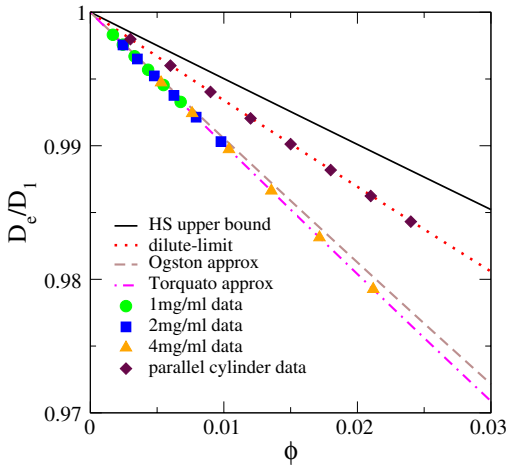

Figure 9. The dimensionless effective diffusion coefficient D_e/D_1 for the collagen networks at different collagen concentrations as a function of the fiber volume fraction. The HS upper bound and various analytical approximations as discussed in section 3.1 are shown and compared to the simulation data.

be seen that the low-density approximation also overestimates D_e for the collagen networks. This is because it considers only the effect of a single long fiber to the diffusing particles. In the actual networks, the average fiber length is less than twice the average pore size as we indicated earlier. Moreover, the cross links also significantly hinder the diffusion of the particles. However, for the parallel-cylinder model at low volume fractions, the low-density approximation should provide accurate estimates, since in such cases, the diffusion of the particles is only hindered by well-separated single cylinders. Indeed, we find that the approximation agrees very well with our simulation data, which also verifies the accuracy of our simulations.

The Ogston approximation that incorporates the pore-size information of the networks provides a much better estimate of D_e compared to the HS bound and the low-density approximation. However, it still slightly overestimates D_e for large particles in networks at high collagen concentrations. This is because the 'influence cylinders' (see section 3.1) are associated with individual long fibers and the effects of finite-fiber length and the cross links are still not fully incorporated. On the other hand, one can see that the Torquato approximation agrees extremely well with the simulation data for all volume fractions that we considered. Specifically, in employing equation (26), we have chosen the four-point parameter value such that $\gamma_2/\zeta_2 = -0.925$. Note that this value is very close to the lower bound value -1, which is not very surprising; the networks can be considered as a kind of 'limit' microstructure. This does not mean the actual value of γ_2/ζ_2 is -0.925 if computed with a full knowledge of the associated three-point function S_3 and four-point function S_4, since the value of ζ_2 we used is also an approximation. The success of the Torquato approximation is due to the fact that higher order microstructural information that possibly reflects the effects of the cross links is already taken into account by the four-point parameter γ_2 in the expression (26).

5. Estimating elastic properties of collagen network using cross-property relations

Since effective properties of heterogeneous materials reflect certain microstructural information about the material, it is possible to extract rigorously information about one physical property given an accurate determination of a different effective property obtained either experimentally or theoretically. Such inter-relationships are called *cross-property* relations [23, 56–60]. Rigorous cross-property relations become especially useful if one property is more easily measured than another property.

In this section, we estimate the effective bulk modulus K_e [23] of fluid-saturated collagen networks using the effective diffusion coefficient D_e computed here using the cross-property relations. In particular, Gibiansky and Torquato [56–58] derived a nontrivial rigorous cross-property upper bound K_e^U on the effective bulk modulus K_e of a fluid-saturated porous material with an insulating solid phase given the effective conductivity (equivalent to the effective diffusion coefficient) of the material, i.e.

$$K_e \leqslant K_e^U = K_{1e} - \frac{2\phi_1\phi_2^2 G_2(K_1 - K_2)^2}{a[3a\phi_1 F - 3a - 2\phi_2 G_2]}, \tag{36}$$

where

$$\begin{aligned} a &= \phi_2 K_1 + \phi_1 K_2 + 4G_2/3, \\ K_{1e} &= \phi_1 K_1 + \phi_2 K_2 - \phi_1\phi_2(K_1 - K_2)^2/a, \end{aligned} \tag{37}$$

and ϕ_1 and K_1 are respectively the volume fraction and bulk modulus of the fluid phase; ϕ_2, K_2, G_2 are respectively the volume fraction, bulk modulus and shear modulus of the solid phase. Moreover, the 'formation factor' F in equation (36) is given by

$$F = \frac{1}{\phi_1}\frac{D_1}{D_e}, \tag{38}$$

where D_1 is the diffusion coefficient of the fluid phase and D_e is the effective diffusion coefficient of the porous material.

For the collagen networks considered here, the solid phase corresponds to the collagen fibers. The bulk modulus K_e of fluid-saturated collagen networks at the fiber volume fraction $\phi_2 = 0.005$ has been measured experimentally [61], i.e. $K_e \approx 2500$ Pa. The shear modulus of 'dry' collagen networks (i.e. fiber networks without fluid) has been computed numerically by Lindström *et al* [14], i.e. $G_2 = 24$ Pa. We use $K_2 = 10$ Pa for the 'dry' network and $K_1 = 2$ GPa for the fluid. Using the Torquato approximation for the effective diffusion coefficient D_e, the upper-bound value obtained from inequality (36) is computed, i.e. $K_e^U = 3530$ Pa, which provides a surprisingly good estimate of K_e, given the fact that K_e^U is a rigorous upper bound [23].

6. Conclusions and discussion

In this paper, we have quantitatively characterized the microstructure, the mean survival time τ and the effective diffusion coefficient D_e of collagen type I networks by applying theoretical and computational techniques from the theory of heterogeneous materials. Specifically, we have computed the pore-size probability density function $P(\delta)$ for

the networks. We have also employed a variety of theoretical approximation schemes for the effective conductivity of a two-phase material to estimate the effective diffusion coefficient D_e for the networks. Such estimates include the low-density approximation, the Ogston approximation and the Torquato approximation, all of which incorporate different levels of microstructural information about the networks. The Hashin–Strikman upper bound on D_e and the pore-size lower bound on τ are used as benchmarks to test our results. Moreover, we have generalized efficient first-passage-time techniques for Brownian-motion simulations in suspensions of spheres to the case of network microstructures and computed the associated D_e and τ. We have found a universal curve for τ for the networks at different collagen concentrations and have shown that the Torquato approximation which takes into account higher order microstructural information can provide the most accurate estimate of D_e for all collagen concentrations among the employed approximation schemes. Our work also demonstrates that employing the rich family of theoretical and simulation techniques developed in material sciences to characterize biological systems (e.g., the heterogeneous host microenvironment of tumors) suggested in [27] is a very promising approach worthy of further exploration.

We have found that as the collagen concentration increases, the diffusion of large particles in the collagen network, and thus the ECM, becomes increasingly difficult, making it is easier for the diffusing particles to be trapped by the fibers. This is a major problem associated with any cancer chemotherapy, since drug macromolecules would get trapped by collagen fibers without successfully diffusing to the target site. It is known that a growing malignant tumor constantly modifies the chemical composition of the collagen network composing its ECM [51]. In addition, since a pressure is built up as the tumor grows, the surrounding ECM is pushed and compressed, leading to a higher collagen concentration in tumor ECM than in normal tissues [52–54]. Therefore, it can be expected that the diffusion of drugs to the tumors would be inhibited. More efficient chemotherapies trying to overcome these difficulties are being developed [55].

We also applied a rigorous cross-property upper bound to estimate the effective bulk modulus K_e of collagen networks from a knowledge of the effective diffusion coefficient D_e computed here. The estimated value of K_e agrees well with existing experimental data, given the fact that it is a rigorous upper bound.

In future work, we intend to generalize our simulation techniques and theoretical approaches to investigate the transport properties of tissues with both collagen networks and various types of cells. Specifically, we will focus on the effects of the cell shape and the plasma membrane on the diffusion of macromolecules. In addition, we will model the mechanical behavior of tissues using the well-developed methods for heterogeneous materials. Progress in these studies should deepen our understanding of the effects of the host microenvironment on tumor growth and should lead to better cancer treatment strategies.

In addition, we will apply cross-property relations to estimate other physical properties of collagen networks from a knowledge of the effective diffusive transport properties computed in this paper. In particular, given the latter, we will bound the fluid permeability [59, 60] for the collagen networks studied here.

Acknowledgments

The authors are very grateful to S B Lindström and D Weitz for providing the data of the collagen networks. This project was supported by the National Center for Research Resources and the National Cancer Institute of the National Institutes of Health through Grant number U54CA143 803. The content is solely the responsibility of the authors and does not necessarily represent the official views of the National Cancer Institute or the National Institutes of Health.

Appendix. Intersection volume of a sphere with a cylinder

Consider a sphere with radius R_s centered at the surface of a cylinder with radius R_c; the intersection volume V_I of the sphere and the cylinder for the case $R_c > R_s$ is given by [62]

$$V_I = \frac{2}{3}\pi R_s^3 + \frac{4}{9\sqrt{A}}[K(k)(A-B)(3B-2A) + E(k)A(2A-4B)], \tag{A.1}$$

where $K(k)$ and $E(k)$ are elliptic integrals of the first and second kind, respectively, i.e.

$$K(k) = \int_0^1 \frac{\mathrm{d}z}{\sqrt{(1-z^2)(1-k^2z^2)}}, \qquad E(k) = \int_0^1 \mathrm{d}z \sqrt{\frac{1-k^2z^2}{1-z^2}}, \tag{A.2}$$

and

$$A = 4R_c^2, \quad B = R_S^2, \quad k^2 = B/A. \tag{A.3}$$

Glossary

- *Collagen*. A group of naturally occurring and the most abundant proteins (biopolymers) found in animals, especially in the flesh and connective tissues of mammals.
- *Heterogeneous material*. A material composed of different materials (e.g., a composite) or the same material in a different state (e.g., a polycrystal). The fluid-saturated collagen networks studied here are special heterogeneous materials.
- *Diffusion coefficient*. A proportionality constant between the molar flux due to molecular diffusion and the gradient in the concentration of the species or the driving force for diffusion.
- *Mean survival time*. The average time that a diffusing molecule spends in the fluid phase before it gets trapped at the interface of the collagen fibers assuming a perfectly absorbing interface.

- *Bulk modulus*. A measure of a material's resistance to uniform compression, defined as the ratio of the infinitesimal pressure increase to the resulting relative decrease of the material's volume.
- *Shear modulus*. A measure of a material's resistance to shape deformation by shear stress, defined as the ratio of shear stress to the shear strain.
- *Correlation function*. A statistical descriptor of the microstructure of a heterogeneous material, quantifying the spatial correlations at different points in the microstructure.
- *'Strong-contrast' expansion*. An infinite series expansion of a specific effective property (e.g., the effective conductivity σ_e) of a two-phase heterogeneous material in terms of the contrast between the corresponding properties of the individual phases [23].
- *Padé approximant*. An approximate resummation of an infinite series in powers of some independent variable x that is expressed as rational functions (ratio of polynomials involving powers of x) [23].
- *First-passage time*. The average time that it takes for a diffusing particle to 'jump' directly to a random location on the surface of an imaginary sphere that is centered at the original position of the particle and entirely within the solvent region.
- *Cross-property relation*: an interrelationship that enables one to extract rigorously information about one physical property of a heterogeneous material given an accurate determination of a different property.

References

[1] Kuntz R M and Saltzman W M 1997 Neutrophil motility in extracellular matrix gels: mesh size and adhesion affect speed of migration *Biophys. J.* **72** 1472–80

[2] Lo C M, Wang H B, Dembo M and Wang Y L 2000 Cell movement is guided by the rigidity of the substrate *Biophys. J.* **79** 144–52

[3] Bischofs I B and Schwarz U S 2003 Cell organization in soft media due to active mechanosensing *Proc. Natl Acad. Sci.* **100** 9274–79

[4] Grinnell F 2003 Fibroblast biology in three-dimensional collagen matrices *Trends Cell Biol.* **13** 264–69

[5] Comper W D 1996 *Extracellular Matrix* (Amsterdam: Harwood Academic)

[6] Gevertz J L and Torquato S 2008 A novel three-phase model of brain tissue microstructure *PLoS Comput. Biol.* **4** e1000152

[7] Jain R K 1987 Transport of molecules in the tumor interstitium: a review *Cancer Res.* **47** 3039–51

[8] Yang Y L, Motte S and Kaufman L J 2010 Pore size variable collagen gels and their interaction with glioma cells *Biomaterials* **31** 5678–88

[9] Ogston A G 1958 The spaces in a uniform random suspension of fibres *Trans. Faraday Soc.* **54** 1754–57

[10] Ogston A G, Preston B N and Wells J D 1973 On the transport of compact particles through solutions of chain-polymers *Proc. R. Soc.* A **333** 297–316

[11] Takahashi A R *et al* 2003 Real space observation of three-dimensional network structure of hydrated fibrin gel *Colloid Polym. Sci.* **281** 832–38

[12] Kaufman L C *et al* 2005 Glioma expansion in collagen I matrices: analyzing collagen concentration-dependent growth and motility patterns *Biophys. J.* **89** 635–50

[13] Mickel W *et al* 2008 Robust pore size analysis of filamentous networks from three-dimensional confocal microscopy *Biophys. J.* **95** 6072–80

[14] Lindström S B, Vader D A, Kulachenko A and Weitz D A 2010 Biopolymer network geometries: characterization, regeneration, and elastic properties *Phys. Rev.* E **82** 051905

[15] Johansson L, Skanzte U and Löfroth J E 1991 Diffusion and interaction in gels and solutions: II. Experimental results on the obstruction effect *Macromolecules* **24** 6019–23

[16] Johansson L, Hedberg P and Löfroth J E 1993 Diffusion and interaction in gels and solutions: IV. Hard sphere Brownian dynamics simulations *J. Phys. Chem.* **97** 747–55

[17] Johansson L and Löfroth J E 1991 Diffusion and interaction in gels and solutions: I. Method *Colloid Interface Sci.* **142** 116–20

[18] Johansson L, Elvingson C and Löfroth J E 1991 Diffusion and interaction in gels and solutions: III. Theoretical results on the obstruction effect *Macromolecules* **24** 6024–9

[19] Johansson L and Löfroth J E 1993 Diffusion and interaction in gels and solutions: V. Nonionic micellar systems *J. Phys. Chem.* **98** 7471–9

[20] Leddy H A, Haider M A and Guilak F 2006 Diffusional anisotropy in collagenous tissues: fluorescence imaging of continuous point photobleaching *Biophys. J.* **91** 311–16

[21] Erikson A *et al* 2008 Physical and chemical modifications of collagen gels: impact on diffusion *Biopolymers* **89** 135–43

[22] Stylianopoulos T, Diop-Frimpong B, Munn L L and Jain R K 2010 Diffusion anisotropy in collagen gels and tumors: the effect of fiber network orientation *Biophys. J.* **99** 3119–28

[23] Torquato S 2002 *Random Heterogeneous Materials: Microstructure and Macroscopic Properties* (New York: Springer)

[24] Sahimi M 2003 *Heterogeneous Materials: Vol 1. Linear Transport and Optical Properties* (New York: Springer)

[25] Sahimi M 2003 *Heterogeneous Materials: Vol 2. Nonlinear and Breakdown Properties, and Atomistic Modelling* (New York: Springer)

[26] Zohdi T I and Wriggers P 2005 *Introduction to Computational Micromechanics* (New York: Springer)

[27] Torquato S 2011 Toward an Ising model of cancer and beyond *Phys. Biol.* **8** 015017

[28] Jiao Y, Berman H, Kiehl T and Torquato S 2011 Spatial organization and correlations of cell nuclei in brain tumors *PLoS One* **6** e27323

[29] Torquato S 1984 Bulk properties of two-phase media: I. Cluster expansion for the dielectric constant of dispersions of fully penetrable spheres *J. Chem. Phys.* **81** 5079–88

[30] Torquato S 1985 Bulk properties of two-phase disordered media: II. Effective conductivity of a dilute dispersion of penetrable spheres *J. Chem. Phys.* **83** 4776–85

[31] Torquato S 1986 Bulk properties of two-phase disordered media: III. New bounds on the effective conductivity of dispersions of penetrable spheres *J. Chem. Phys.* **84** 6345–59

[32] Lado F and Torquato S 1986 Effective properties of two-phase disordered composite media: I. Simplification of bounds on the conductivity and bulk modulus of dispersions of impenetrable spheres *Phys. Rev.* B **33** 3370–78

[33] Lado F and Torquato S 1986 Effective properties of two-phase disordered composite media: II. Evaluation of bounds on the conductivity and bulk modulus of dispersions of impenetrable spheres *Phys. Rev.* B **33** 6428–34

[34] Beasley J D and Torquato S 1986 Bounds on the conductivity of a suspension of random impenetrable spheres *J. Appl. Phys.* **60** 3576–81

[35] Torquato S and Lado F 1988 Bounds on the effective transport and elastic properties of cylindrical fibers in a matrix *J. Appl. Mech.* **55** 347–54
[36] Miller C A and Torquato S 1991 Diffusion-controlled reactions among spherical traps: effect of polydispersivity in trap size *J. Appl. Phys.* **69** 1948–55
[37] Lado F and Torquato S 1990 Two-point probability function for distributions of oriented hard ellipsoids *J. Chem. Phys.* **93** 5912–17
[38] Coker D, Torquato S and Dunsmuir J 1996 Morphological and physical properties of Fountainebleu sandstone from tomographic analysis *J. Geophys. Res.* **101** 17497–506
[39] Torquato S, Yeong C, Rintoul M D, Milius D and Aksay I A 1999 Characterizing the structure and mechanical properties of interpenetrating multiphase cermets *J. Am. Ceram. Soc.* **82** 1263–68
[40] Torquato S and Avellaneda M 1991 Diffusion and reaction in heterogeneous media: pore size distribution, relaxation times, and mean survival time *J. Chem. Phys.* **95** 6477–89
[41] Torquato S 1985 Effective electrical conductivity of two-phase disordered composite media *J. Appl. Phys.* **58** 3790–97
[42] Hashin Z and Strikman S 1962 A variational approach to the theory of the effective magnetic permeability of multiphase materials *J. Appl. Phys.* **33** 3125–32
[43] Prager S 1963 Interphase transfer in stationary two-phase media *Chem. Eng. Sci.* **18** 227–31
[44] Torquato S and Kim I C 1989 Efficient simulation technique to compute effective properties of heterogeneous media *Appl. Phys. Lett.* **55** 1847–49
[45] Kim I C and Torquato S 1990 Determination of the effective conductivity of heterogeneous media by Brownian motion simulation *J. Appl. Phys.* **68** 3892–903
[46] Kim I C and Torquato S 1991 Effective conductivity of suspensions of hard spheres by Brownian motion simulation *J. Appl. Phys.* **69** 2280–89
[47] Kim I C and Torquato S 1992 Diffusion of finite-sized Brownian particles in porous media *J. Appl. Phys.* **71** 2727–35
[48] Kim I C and Torquato S 1992 Diffusion of finite-sized Brownian particles in porous media *J. Chem. Phys.* **96** 1498–503
[49] Torquato S 1991 Trapping of finite-sized Brownian particles in porous media *J. Chem. Phys.* **95** 2838–41
[50] Torquato S and Yeong C L Y 1997 Universal scaling for diffusion-controlled reactions among traps *J. Chem. Phys.* **106** 8814–20
[51] Hanahan D and Weinberg R A 2000 The hallmarks of cancer *Cell* **100** 57–70
[52] Helmlinger G, Netti P A, Lichtenbeld H C, Melder R J and Jain R K 1997 Solid stress inhibits the growth of multicellular tumor spheroids *Nature Biotech.* **15** 778–83
[53] Jiao Y and Torquato S 2012 Diversity of dynamics and morphologies of invasive solid tumors *AIP Adv.* **2** 011003
[54] Jiao Y and Torquato S 2011 Emergent behaviors from a cellular automaton model for invasive tumor growth in heterogeneous microenvironments *PLoS Comput. Biol.* **7** e1002314
[55] Joensuu H 2008 Systemic chemotherapy for cancer: from weapon to treatment *Lancet Oncol.* **9** 304
[56] Gibiansky L V and Torquato S 1993 Link between the conductivity and elastic moduli of composite materials *Phys. Rev. Lett.* **71** 2927–30
[57] Gibiansky L V and Torquato S 1996 Link between the conductivity and elastic moduli of composite materials *Proc. R. Soc.* A **452** 253–83
[58] Gibiansky L V and Torquato S 1998 Rigorous connection between physical properties of porous rocks *J. Geophys. Res.* **103** 23911–23
[59] Torquato S 1990 Relationship between permeability and diffusion-controlled trapping constant of porous media *Phys. Rev. Lett.* **64** 2644–46
[60] Avellaneda M and Torquato S 1991 Rigorous link between fluid permeability, electrical conductivity, and relaxation times for transport in porous media *Phys. Fluids* A **3** 2529–40
[61] Raub C B, Putnama A J, Tromberg B J and George S C 2010 Predicting bulk mechanical properties of cellularized collagen gels using multiphoton microscopy *Acta Biomaterialia* **6** 4657–65
[62] Lamarche F and Leroy C 1990 Evaluation of the volume of intersection of a sphere with a cylinder by elliptic integrals *Comput. Phys. Commun.* **59** 359–69